Post-process wavelength tuning of silicon photonic crystal slow-light waveguides

Kashif M. Awan,[1] Sebastian A. Schulz,[2] Dennis X. Liu,[2] Ksenia Dolgaleva,[1] Jeremy Upham,[2,*] and Robert W. Boyd[1,2,3]

[1]*School of Electrical Engineering and Computer Science, University of Ottawa, 25 Templeton, Ottawa, ON, K1N 6N5, Canada*

[2]*Department of Physics, University of Ottawa, 25 Templeton, Ottawa, ON, K1N 6N5, Canada*

[3]*The Institute of Optics, University of Rochester, Rochester New York 14627, USA*

**Corresponding author: jupham@uottawa.ca*

Received January 5, 2015; revised March 26, 2015; accepted March 26, 2015; posted March 31, 2015 (Doc. ID 231788); published April 21, 2015

Silicon photonic crystal waveguides have enabled a range of technologies, yet their fabrication continues to present challenges. Here, we report on a post-processing method that allows us to tune the operational wavelength of slow-light photonic crystal waveguides in concert with optical characterization, offsetting the effects of hole-radii and slab thickness variations. Our method consist of wet chemical surface oxidation, followed by oxide stripping. Theoretical modelling shows that the changes in optical behavior were predictable, and hence controlled tuning can be achieved by changing the number of processing cycles, where each cycle removes approximately 0.25 nm from all exposed surfaces, producing a blueshift of 1.6±0.1 nm in operating wavelength. © 2015 Optical Society of America

OCIS codes: (230.5298) Photonic crystals; (130.5296) Photonic crystal waveguides; (220.4241) Nanostructure fabrication.

http://dx.doi.org/10.1364/OL.40.001952

Two-dimensional photonic crystals (PC) take advantage of their photonic band gap and the engineering of defect modes within it to form low-loss nanophotonic components [1–10]. These components include optical resonators with large quality factors and sub-wavelength cubed modal volumes [6,11], high confinement slow-light waveguides [12], and precise control over dispersion [13–15]. Significant efforts [16–18] have gone into the development of fabrication processes that faithfully reproduce the PC designs. Particular attention has gone into refinements of the e-beam lithography processes [19] and plasma etching [17] stages, to limit both the offsets and random variations of hole size, shape, and position, as well as sidewall roughness. Despite such efforts, certain deviations are inevitable in fabricated samples, such as variation in substrate thickness [20] and run-to-run differences during fabrication, leading to systematic hole-radii deviations, that result in a shift of the operating wavelength [21]. These variations necessitate a broad range of lithography doses, hole sizes, and lattice constants to be written on each sample to ensure that even a single device can be optically characterized at the intended wavelengths. Obtaining a device at the correct operation wavelength is particularly important for slow-light PC waveguides because dispersion engineering to increase the slow-down factor of a waveguide will consequently decrease the bandwidth over which slow-light can be observed [14].

This work investigates the use of inexpensive wet etching steps as a post-processing technique to tune the operating wavelength of slow-light PC waveguides in a silicon substrate. Similar post-processing approaches have been applied to devices made with III–V semiconductor substrates [22] as well as in silicon PC nanocavities [23]. Our work demonstrates that this approach can predictably blue shift the inherently narrow bandwidth of silicon slow-light PC waveguides to a desired operating wavelength. Tuning to the desired operating wavelength through optical characterization and post-processing significantly reduces the necessary size of parameter sweeps, shortening expensive write times, accelerating device development, such as delay lines or four wave mixing waveguides for optical signal processing, and most importantly increasing the yield of devices with slow-light waveguides per process run.

The post-processing method used for controlled removal of Si layers from the surfaces of the PC device provides a consistent reduction of the slab thickness and enlargement of air-holes. Both these modifications contribute to a blue shift of the slow-light region. The process is based on previous work by Song *et al.* [23] on PC nanocavities. As a first step, the outer layer of Si is oxidized, resulting in the formation of thin SiO_2 layer that is subsequently removed by a selective wet etching.

Oxidation is performed by immersion in a solution of 1 part 30% Hydrogen peroxide (H_2O_2) and 8 parts water (20°C) for 60 s, then rinsed in deionized water (20°C) for 60 s and dried by N_2. To selectively etch the oxidized surface of the device, i.e., the SiO_2, the device is placed in dilute hydrofluoric acid (1% HF, 20°C) for 180 s then rinsed in deionized water and dried with N_2 as before. Figure 1 shows a schematic of a single post-processing H_2O_2-HF cycle. Repetition of the whole cycle removes additional Si layers and results in further blue shift of the slow-light region.

To experimentally test this approach, we fabricated slow-light PC waveguides in Si, based on a W1 dispersion engineered waveguide with a lattice constant (a) of 416 nm, a typical air hole radius of 123.6 nm ($0.297a$), and shifting of the nearest and next-nearest hole rows to the line defect waveguide along the direction of the line defect by −40 nm ($-0.096a$) and 8 nm ($0.019a$), respectively. The PC waveguides were fabricated on a SOITEC silicon-on-insulator wafer comprising a 210-nm-thick Si layer on 2 μm of silica. The pattern was exposed on ZEP520A electron beam resist using a 30-keV RAITH

 © 2015 Optical Society of America

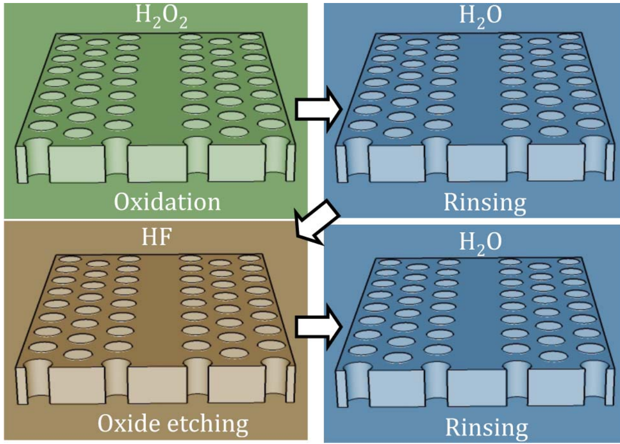

Fig. 1. Schematic of the post-processing steps on a PC waveguide. Oxidation is performed using H_2O_2, followed by a water rinse. To etch the oxidized layer, diluted HF was used followed by a second water rinse.

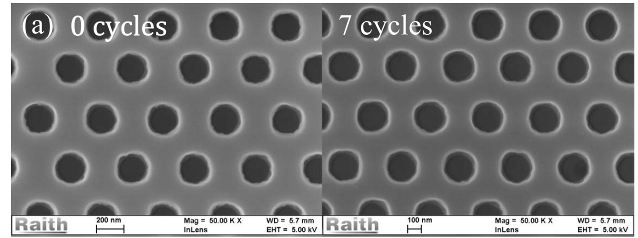

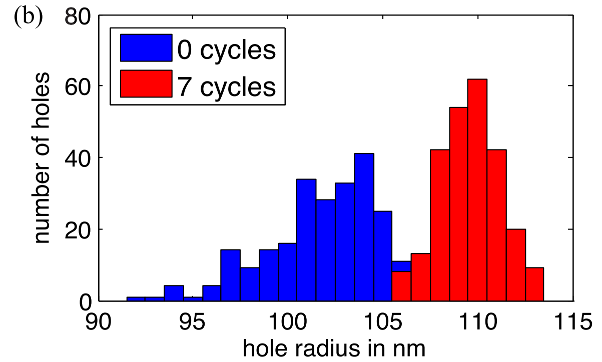

Fig. 2. (a) Scanning electron microscope (SEM) images of PC holes before and after 7 post-processing cycles. Both images were taken at 50-k magnification. (b) A comparison of hole radii from such images suggests an increased hole-radius after wet chemical etching, which is supported by statistical analysis across multiple such images.

electron beam writer and subsequently was transferred into the silicon layer using electron cyclotron resonance (ECR) etching with a fluorine-based chemistry. Free-standing PC waveguides were created by removing the buried silica beneath the photonic crystal using HF. Subsequently, for post-processing, the device undergoes the post-processing cycle outlined in Fig. 1. This process results in removal of silicon from all of the device surfaces, hence resulting in a reduction of slab thickness as well as increment of hole radii.

We characterize this change in hole-radii by inspecting approximately 250 holes with a scanning electron microscope (SEM) before and after 7 post-processing cycles. Figure 2 shows exemplary SEM images of the PC air holes before post-processing and after 7 cycles of the process along with statistical hole-radii analysis. This analysis confirms the removal of silicon due to our H_2O_2-HF process as the average hole-radius increases from 102 to 110 nm after 7 H_2O_2-HF cycles. This increase is significantly larger than the variation of radii for each set of SEM images (the standard deviation of radii is 3.00 nm and 1.56 nm for 0 and 7 cycles, respectively). The reduction in the standard deviation after 7 cycles suggest an improvement in the uniformity of the air holes.

Group index measurements for these devices were performed experimentally via Fourier transform spectral interferometry. A schematic of the characterisation set-up is shown in Fig. 3(a), which consists of a Mach–Zehnder interferometer with the slow-light PC in one arm. The transmitted light is resolved using an optical spectrum analyzer (OSA) [24]. Figure 3(b) shows group index measurements for the same PC waveguide device after 0, 2, 5, and 7 H_2O_2-HF cycles. Each cycle blue shifts the operating wavelength by 1.6 ± 0.1 nm, except for the first cycle, which results in a more pronounced shift. The first cycle also removes residues from resists, any native oxide that has grown during storage of the wafer, and other impurities, hence leading to a larger shift of 4.9 ± 0.2 nm. The group index spectrum after 7 cycles shows some increase in noise as the grating couplers used to couple light from optical fibre into the waveguides showed a reduction in transmission power as they were blue-shifted by post-processing. Such a reduction in transmission could be resolved by selecting the starting grating coupler design to target the intended operating wavelength, as they have a bandwidth of at least 35 nm [25]. It is also evident from Fig. 3 that post-processing cycles increase the slope of the dispersion curve. To understand this further, modelling of the characterized PC waveguides was carried out using the MIT plane wave band solver MPB [26].

The photonic bandgap simulations for each case were performed in 3 dimensions using MPB. For the initial, ‘As etched’ case, the hole radius was set to 123.6 nm and the slab thickness to 210 nm, consistent with the design of the fabricated device. The dashed line overlapping the ‘As etched’ experimental curve in Fig. 3 shows that the theoretical and experimental data match, without any free parameters. To model the device response after 2 cycles of post-processing, the hole radius was increased by 1.5 nm, and the slab thickness was reduced by 3 nm. For all subsequent cases, the hole radius was increased by 0.25 nm, and the slab thickness was reduced by 0.5 nm per cycle. Again, no free fitting parameters were required to match the simulated group index curves to the measured results shown in Fig. 3. The simulations accurately reproduce both the shift in the operating wavelength and changes in the shape of the group index curves, suggesting that, except for the first cycle, each H_2O_2-HF cycle removed on average 0.25 nm from all exposed surfaces of the silicon PC. Given that the lattice constant of crystalline silicon is 0.54 nm and the nearest neighbor separation between silicon atoms is 0.23 nm [27], this suggests that, on average, a monolayer of silicon is being removed per cycle.

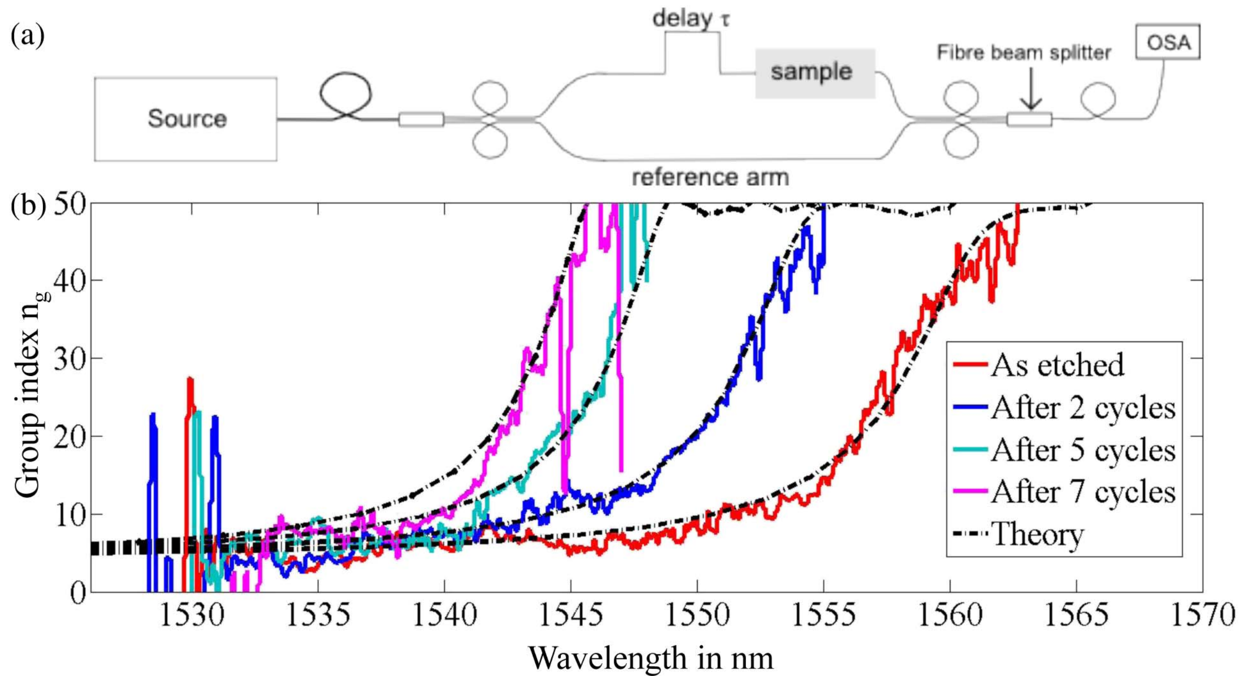

Fig. 3. Experimental confirmation of operational wavelength shift. (a) Schematic of characterization set-up. (b) Comparison of theoretical (dashed lines) and experimental (solid lines) group index curves for a slow-light photonic crystal waveguide after 0, 2, 5, and 7 H_2O_2-HF cycles. The slab thickness and hole-radius were varied correspondingly, starting from the as-fabricated design, to obtain the theoretical curves for 2, 5, and 7 cycles, while all other parameters were held constant. This confirms that this process can be used to tune the operating wavelength as per requirement by varying the number of cycles.

We demonstrate that a simple wet chemical process consisting of controlled oxidation and subsequent oxide removal can be used to stepwise tune the operating wavelength of slow-light PC waveguides after device fabrication and initial optical characterization. Repeat cycles of this post-processing procedure can be used to achieve precise control of the final operating wavelength of PC waveguides since each cycle blue shifts the operating wavelength by 1.6 ± 0.1 nm, excluding the first cycle. Such a blue shift is consistent with the removal of silicon during the chemical etching, and our theoretical modelling confirms this behavior. The excellent agreement between theoretical and experimental data indicates that it is possible to predetermine the number of processing cycles required to shift a device to the desired wavelength. In principle, cycles could be repeated until the suspended structure collapses. Of course, as with dose sweeps, shifting of the operational bandwidth by this post-processing will slightly change the performance of the device. However, because the silicon removal process is uniform across all surfaces, this change is utterly predictable and can be incorporated into the design so that device operation is not compromised while shifting the operational bandwidth. This simple method reduces the impact of variations in the slab thickness or systematic deviations of the hole-radius during fabrication, hence increasing the yield of slow-light PC waveguide fabrication. Initial evidence shows an improvement in the hole uniformity, suggesting that further investigation may be able to quantify the influence of different disorder sources (e.g., surface roughness versus hole size disorder) on propagation loss in slow-light PC waveguides [28–33].

The authors would like to thank Robert Vandusen for fruitful discussions during device fabrication and acknowledge the support of the Canada Excellence Research Chairs (CERC) Program.

References

1. S. John, Appl. Phys. Lett. **58**, 2486 (1987).
2. E. Yablonovitch, Appl. Phys. Lett. **58**, 2059 (1987).
3. T. F. Krauss, R. M. De La Rue, and S. Brand, Nature **383**, 699 (1996).
4. M. Lončar, D. Nedeljković, T. Doll, J. Vučković, A. Scherer, and T. P. Pearsall, Appl. Phys. Lett. **77**, 1937 (2000).
5. S. Noda, A. Chutinan, and M. Imada, Nature **407**, 608 (2000).
6. Y. Akahane, T. Asano, B. S. Song, and S. Noda, Nature **425**, 944 (2003).
7. B. S. Song, T. Asano, Y. Akahane, and S. Noda, Phys. Rev. B **71**, 195101 (2005).
8. T. F. Krauss, Nat. Photonics **2**, 448 (2006).
9. T. Baba, Nat. Photonics **2**, 465 (2008).
10. T. F. Krauss, J. Phys. D **40**, 2666 (2007).
11. B. S. Song, T. Asano, S. Noda, and Y. Akahane, Nat. Mater. **4**, 207 (2005).
12. M. Notomi, K. Yamada, A. Shinya, J. Takahashi, C. Takahashi, and I. Yokohama, Phys. Rev. Lett. **87**, 253902 (2001).
13. L. H. Frandsen, A. V. Lavrinenko, J. Fage-Pedersen, and P. I. Borel, Opt. Express **14**, 9444 (2006).
14. J. Li, T. P. White, L. O'Faolain, A. Gomez-Iglesias, and T. F. Krauss, Opt. Express **16**, 6227 (2008).
15. S. A. Schulz, L. O'Faolain, D. M. Beggs, T. P. White, A. Melloni, and T. F. Krauss, J. Opt. **12**, 104004 (2010).
16. E. Kuramochi, M. Notomi, S. Hughes, A. Shinya, T. Watanabe, and L. Ramunno, Phys. Rev. B **72**, 161318 (2005).
17. L. O'Faolain, X. Yuan, D. Mcintyre, S. Thoms, H. Chong, R. M. De La Rue, and T. F. Krauss, Electron. Lett. **42**, 1454 (2006).

18. T. Asano, B. S. Song, and S. Noda, Opt. Express **14**, 1996 (2006).
19. J. Li, L. O'Faolain, S. A. Schulz, and T. F. Krauss, Photonics Nanostruct. Fundam. Appl. **10**, 589 (2012).
20. G. Celler and M. Wolf, "Smart Cut A guide to the technology, the process, the products" (2003). http://www.soitec.com/pdf/SmartCut_WP.pdf
21. D. M. Beggs, L. O'Faolain, and T. F. Krauss, Photonics Nanostruct. Fundam. Appl. **6**, 213 (2008).
22. K. Hennessy, A. Badolato, A. Tamboli, P. M. Petroff, E. Hu, M. Atature, J. Dreiser, and A. İmamoğlu, Appl. Phys. Lett. **87**, 021108 (2005).
23. B. S. Song, T. Nagashima, T. Asano, and S. Noda, Appl. Opt. **48**, 4899 (2009).
24. A. Gomez-Iglesias, D. O'Brien, L. O'Faolain, A. Miller, and T. F. Krauss, Appl. Phys. Lett. **90**, 261107 (2007).
25. D. Taillaert, P. Bienstman, and R. Baets, Opt. Lett. **29**, 2749 (2004).
26. S. Johnson and J. Joannopoulos, Opt. Express **8**, 173 (2001).
27. N. W. Ashcroft and N. D. Mermin, *Solid State Physics* (Brooks/Cole, 1976), Chap. 4.
28. S. Hughes, L. Ramunno, J. F. Young, and J. E. Sipe, Phys. Rev. Lett. **94**, 033903 (2005).
29. S. Johnson, M. Povinelli, M. Soljačić, A. Karalis, S. Jacobs, and J. Joannopoulos, Appl. Phys. B **81**, 283 (2005).
30. L. O'Faolain, T. P. White, D. O'Brien, X. Yuan, M. D. Settle, and T. F. Krauss, Opt. Express **15**, 13129 (2007).
31. B. Wang, S. Mazoyer, J. P. Hugonin, and P. Lalanne, Phys. Rev. B **78**, 245108 (2008).
32. M. Patterson, S. Hughes, S. Combrie, N.-V.-Q. Tran, A. D. Rossie, R. Gabet, and Y. Jaouen, Phys. Rev. Lett. **102**, 253903 (2009).
33. L. O'Faolain, S. A. Schulz, D. M. Beggs, T. P. White, M. Sapsenovic, L. Kuipers, F. Morichetti, A. Melloni, S. Mazoyer, J. P. Hugonin, P. Lalanne, and T. F. Krauss, Opt. Express **18**, 27627 (2010).

197.122.64.31 {ts '2018-10-22 10:35:03'}